Dynamics of Boundedly Rational Monopoly with Time Delay*

Akio Matsumoto† Chuo University

Ferenc Szidarovszky‡ University of Arizona

Abstract

The purpose of this paper is to study dynamics of a monopolistic firm in a continuous-time framework. The firm is assumed to be boundedly rational implying that it can obtain only limited information and experience delay information on demand. A dynamic adjustment process is based on the gradient of the expected profit. It is analytically demonstrated that a monopoly equilibrium undergoes a Hopf bifurcation when it loses stability. Global dynamic behavior is confirmed by numerical simulations.

1 Introduction

In the recent literature, it has been recognized in continuous-time economic dynamics that a delay differential system is useful to describe the periodic and aperiodic behavior of economic variables. Time delays can be modeled in two different ways: fixed-time delays and continuously distributed time delays. Invernizzi and Medio (1991) investigate various economic models with the latter and confirm analytically as well as numerically the conditions for chaotic solution. On the other hand Matsumoto (2009) reconstructs Goodwin's accelerator model with the former as a delay neutral differential equation and examine the condition under which multiple limit cycles coexist. More recently, Matsumoto and Szidarovszky (2011a) introduce a production delay of both types and a mound-shaped production function into the neoclassical one-sector growth model and show the birth of complex dynamics. With the infinite dimensionality created

*The authors highly appreciate finanical supports from Chuo University (Joint Research Grant 0981), the Japan Society for the Promotion of Science (Grant-in-Aid for Scientific Research (C) 21530172) and the Japan Economic Research Foundation. The research leading to this paper started when the first author visited the Department of Systems and Industrial Engineering of the University of Arizona and finished when the second author visited the Department of Economics, Chuo University. They appreciated hospitalities of those universities over their stay. The usual disclaimer applies.

†Department of Economics, Chuo University, 742-1, Higashi-Nakano, Hachioji, Tokyo, 192-0393, Japan. akiom@tamacc.chuo-u.ac.jp

‡Department of Systems and Industrial Engineering, University of Arizona, Tucson, Arizona, 85721-0020, USA. szidar@sie.arizona.edu

by a fixed-time delay, even a single first-order equation is transformed into an equation with a sufficient number of degrees of freedom to permit the occurrence of complex dynamics involving chaotic phenomena. This finding indicates that fixed delay models of a dynamic economy may explain various complex dynamic behavior of the economic variables.

This study is an application of Matsumoto and Szidarovszky (2011b) where a complete eigenvalue analysis is given for a certain class of differential equations with a single delay. In particular, it considers monopoly dynamics with a fixed time delay. It is well known that traditional monopoly market has such a structure in which there is only one seller, called a monopolistic firm or a monopoly, and there are infinitely many small buyers whose behavior is described by the market demand function. Further, the firm is assumed to be *rational* in a sense that full information or knowledge on demand is available free of charge without any delays. As a result, it is enough for the firm to determine either price or quantity (but not both) so as to maximize profit. Once one of price or quantity is chosen, then the other is automatically determined through the demand function. No matter which choice is made, it can jump to the same optimum point in one shot without any adjustment considerations. In reality, however, the monopolistic firm has only limited information, usually obtains price information and sales data with some delays and reacts cautiously. Getting closer to the real world and making the monopoly theory more convincing, we replace this extreme assumption with the more plausible behavior assumption in which full and instantaneous information is eliminated. Indeed it is assumed first that the monopolistic firm knows only a few points on the demand function (i.e., partial information). Second it is assumed that the firm experiences time delays inherent in phenomena like information and implementation delays (i.e., delay information). Such a firm is called *boundedly rational*. A natural consequence of alternating behavioral assumptions is that the firm is not able to arrive at the optimal point with one shot but gropes for it. In addition to this, dynamics of a delay differential monopoly with the gradient method has not yet been revealed in the existing literature. Therefore, in this study, we draw our attention to dynamics of a continuous-time and fixed-delay monopoly under a circumstance where a firm is boundedly rational and uses the gradient of the expected profit to revise its output decision.[1]

The paper is organized as follows. Section 2 is divided into two parts. In the first part, a gradient dynamic monopoly model with time delay is constructed and then local stability is considered. It the second part, numerical simulations are given to confirm global stability of a unstable monopoly equilibrium. Section 3 concludes the paper.

[1] Concerning discrete-time monopoly dynamics, we mention Puu (2003) and Naimzada (2011). The former assumes bounded rationality and shows that the monopolistic firm behaves in an erratic way. The latter exhibits that fixed delay dynamics of the monopoly with bounded rationality can be described by the well-known logistic equation when the firm takes a learning activity of revising decisions.

2 Delay Monopoly

Consider optimal behavior of a boundedly rational monopolistic firm which produces output denoted by q with marginal cost c. The price function is assumed to be linear

$$f(q) = a - bq,\ a,\ b > 0.$$

We confine attention to a situation where the firm does not know the price function and does not even know that it is linear. It is however able to estimate its derivative using actual prices it received in the past. By using numerical differentiation, it is able to estimate the derivative at a value q^e of output which is believed to be close to the actual output it would select. The estimated derivative value is

$$\frac{d\pi^e}{dq^e} = a - c - 2bq^e.$$

So the approximating gradient dynamics is

$$\dot{q} = \alpha(q)\frac{d\pi^e}{dq^e} \tag{1}$$

where $\alpha(q)$ is an adjustment function. In constructing best response dynamics, global information is required about the profit function, however, in applying gradient dynamics, only local information is needed. We make the familiar assumption that the adjustment function has linear dependency on output:

Assumption 1. $\alpha(q) = \alpha q$ with $\alpha > 0$.

The gradient dynamics under Assumption 1 with an expected output is presented by

$$\dot{q}(t) = \alpha q(t)\left[a - c - 2bq^e(t)\right] \tag{2}$$

where t denotes a point of continuous time.

2.1 Single Fixed-Delay

Dynamics depends on the formation of expectations. We consider a simple case in which at time t, the firm forms its expected demand to be equal to realized demand at time $t - \tau,\ \tau > 0$. Since it can be supposed that the actual output produced at time $t - \tau$ is equal to demand, the expected demand is given in terms of output:

Assumption 2 $q^e(t) = q(t - \tau)$.

Replacing $q^e(t)$ in equation (2) with $q(t-\tau)$, we obtain the output adjustment process as a nonlinear differential equation with one fixed-time delay

$$\dot{q}(t) = \alpha q(t)\left[a - c - 2bq(t - \tau)\right]. \tag{3}$$

Equation (3) has two stationary points; a trivial point $q(t) = 0$ and a non-tirival point

$$q^M = \frac{a-c}{2b}$$

where $a > c$ is assumed to ensure a positive stationary output. We may call q^M a monopoly equilibrium.

Our first concern is upon local stability of q^M. For this purpose, we analyze the linearized version of (3) about the monopoly equilibrium. Linearization and introduction of the new variable $q_\delta(t) = q(t) - q^M$ reduce equation (3) to

$$\dot{q}_\delta(t) = -\gamma q_\delta(t-\tau) \text{ with } \gamma = \alpha(a-c) > 0, \tag{4}$$

which has the zero-solution, $q_\delta(t) = 0$ (or $q(t) = q^M$) for all $t \geq 0$. If there is no time delay, $\tau = 0$, then equation (4) becomes an ordinary differential equation and has a stable solution, $q_0 e^{-\gamma t}$, where q_0 is an initial point. If there is a positive time delay, $\tau > 0$, then equation (4) becomes a linear delay differential equation where initial data are given by a continuous function defined for $-\tau \leq t \leq 0$. It is impossible to derive an explicit solution even though the equation seems to be simple. In spite of this inconvenience, it is possible to analyze qualitative aspects of the solution in the following way. Substituting the exponential solution $q_\delta(t) = q_0 e^{\lambda t}$ into (4) yields the characteristic equation associated with the linearized delay equation

$$\lambda + \gamma e^{-\lambda\tau} = 0. \tag{5}$$

The sufficient condition for local asymptotical stability of the zero-solution is that the real parts of the eigenvalues are negative.

The characteristic equation is a function of τ and so are its roots. Since the monopoly equilibrium is asymptotically stable for $\tau = 0$, we expect, by continuity, that the equilibrium remains asymptotically stable with positive but small values of τ. To examine the location of the roots, we multiply both sides of equation (5) by τ and introduce the new variables, $x = \lambda\tau$ and $A = \lambda\tau$. Then equation (5) is simplified to be

$$x + Ae^{-x} = 0. \tag{6}$$

Real roots of equation (6) can be checked by a graphical method using the two functions,

$$y_1 = -\frac{x}{A} \text{ and } y_2 = e^{-x}.$$

Real roots correspond to intersections of these functions. Depending on the value of A, the two functions have two, one and zero intersections implying that equation (6) has two, one or no real roots. Consider the condition needed for the straight line to be tangent to the exponential curve. As is seen in Figure 1, let us denote the tangency point by $P = (\bar{x}, \bar{y})$ at which the following two

conditions are satisfied:

$(i) -\dfrac{1}{A} = -e^{-\bar{x}}$: the slopes of the two functions are equal;

$(ii) -\dfrac{\bar{x}}{A} = e^{-\bar{x}}$: the ordinates of the two functions for $x = \bar{x}$ are equal.

From (i) and (ii), $\bar{x} = -1$. Therefore $A = 1/e$ is the tangency condition and equation (6) has two distinct real roots if $A < 1/e$ and a pair of conjugate complex roots if $A > 1/e$.

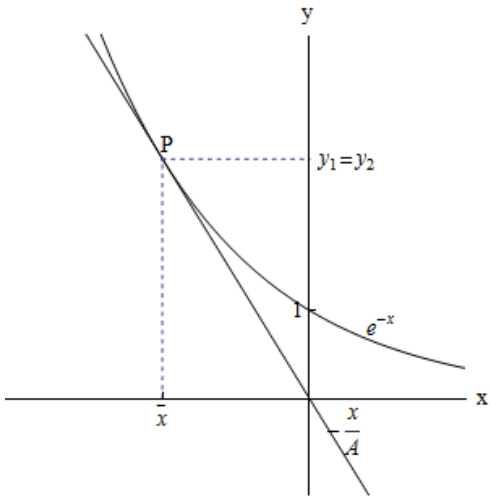

Figure 1. Tangency condition

Assume that $x = \alpha + i\beta$ with $\beta > 0$.[2] Substituting this root in equation (6) and arranging the terms give

$$\alpha + Ae^{-\alpha}\cos\beta + i\{\beta - Ae^{-\alpha}\sin\beta\} = 0$$

where the real and imaginary parts should be equal to zero,

$$\alpha + Ae^{-\alpha}\cos\beta = 0 \tag{7}$$

and

$$\beta - Ae^{-\alpha}\sin\beta = 0. \tag{8}$$

If $\sin\beta = 0$, then from equation (8), $\beta = 0$, which implies that the root is real and violates the assumption $\beta > 0$. So we eliminate the case of $\sin\beta = 0$ or

[2] If $\alpha + i\beta$ with $\beta > 0$ is a root, then so also is the one with $\beta < 0$. We consider only the roots with $\beta > 0$.

$\beta = n\pi$ for $n \in N$, the set of integers including zero. On the other hand if $\sin\beta \neq 0$, then from (8),

$$e^{-\alpha} = \frac{\beta}{A\sin\beta}.$$

Substituting it into equation (7) presents

$$\alpha = -\beta\cot\beta \tag{9}$$

which is then substituted into equation (8) to obtain

$$\beta = Ae^{\beta\cot\beta}\sin\beta \tag{10}$$

where the right-hand side is denoted by $f(\beta)$ in the following. The imaginary part of the eigenvalue is a solution of equation (10) and the real part is given by equation (9).[3] We define two intervals of β,

$$\Omega_1 = \cup_{n\in N}\left(n\pi, \frac{\pi}{2} + n\pi\right) \text{ and } \Omega_2 = \cup_{n\in N}\left(\frac{\pi}{2} + n\pi, (1+n)\pi\right)$$

Equation (9) implies that $sign(\alpha) = -sign(\cot\beta)$ where $\cot\beta > 0$ for $\beta \in \Omega_1$ and $\cot\beta < 0$ for $\beta \in \Omega_2$. Thus the real parts are negative for $\beta \in \Omega_1$ and positive for $\beta \in \Omega_2$. Accordingly we call Ω_1 the stable interval and Ω_2 the unstable interval.

We are concerned with the location of β solving equation (10). The graphs of $f(\beta)$ with $A = \pi/2$ and $A = 5\pi/2$ are shown in Figures 2A and 2B where they take a mound-shape profile for $\beta \in (0, \pi)$, furthermore $f'(\beta) > 0$ for $\beta \in ((2n-1)\pi, 2n\pi)$ and $f'(\beta) < 0$ for $\beta \in (2n\pi, (2n+1)\pi)$ for $n \geq 1$.[4] The value of β is an intersection of $f(\beta)$ with the 45° line. Since equation (6) is transcendental, it has infinitely many solutions. In consequence, the number of intersections is also infinite. With the assumption $\beta > 0$, the roots are purely imaginary when $\cot\beta = 0$ or $\beta = \pi/2 + n\pi$. However, to hold $\beta > 0$, $\sin\beta > 0$ is needed from equation (10), so $\alpha = 0$ and $\beta > 0$ only for

$$\beta = \frac{\pi}{2} + 2n\pi.$$

Substituting $\alpha = 0$ and this threshold value of β into equation (8) yields $\beta = A$, which can be written as

$$A = \frac{\pi}{2} + 2n\pi.$$

The determination of β under $A = \pi/2$ (i.e., $n = 0$) is illustrated in Figure 2A where three red dots denote the intersections, e_1, e_2 and e_3. The values of β

[3] There are several ways to solve these two equations for α and β. We outline the two ways, one provided by Frisch and Holme (1935) and the other by Hayes (1950) in the Appendix.

[4] Needless to say, the shape of the graph can be analytically determined. See Matsumoto and Szidarovszky (2011b).

and α are

$$\beta_1^0 = \frac{\pi}{2} \text{ at } e_1 \text{ and } \alpha_1^0 = 0,$$

$$\beta_2^0 \simeq 7.65 < \frac{5\pi}{2} \text{ at } e_2 \text{ and } \alpha_2^0 \simeq -1.60, \tag{11}$$

$$\beta_3^0 \simeq 13.98 < \frac{9\pi}{2} \text{ at } e_3 \text{ and } \alpha_3^0 \simeq -2.20$$

where the upper script indicates the value of n and the subscript corresponds to the numbering of the intersection. Let $x_j^n = \alpha_j^n + i\beta_j^n$, then x_1^0 is a purely imaginary root and the real parts of x_2^0 and x_3^0 are negative implying that β_2^0 and β_3^0 are in Ω_1. Graphically, the intercepts e_2 and e_3 are in the shaded regions of Figure 2(A).

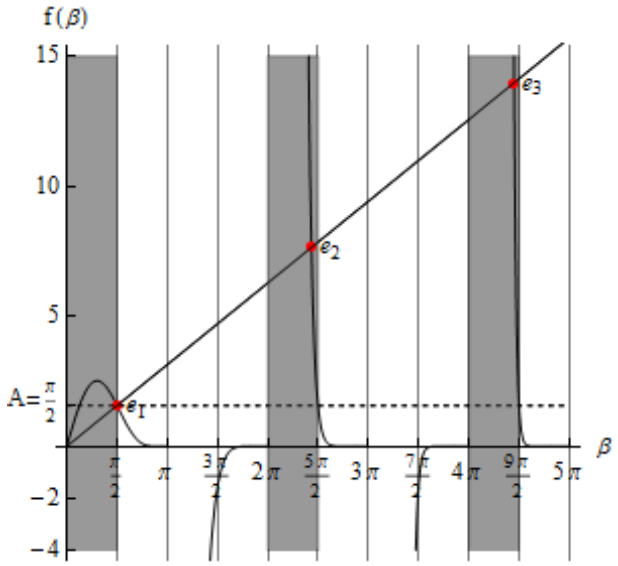

Figure2(A) Determination of β for $A = \pi/2$

If $A < \pi/2$, then the 45° line crosses the $\beta = \pi/2$ vertical line above A, so $\beta_1 < \pi/2$, $\beta_2 < 5\pi/2$ and $\beta_3 < 9\pi/2$ while the corresponding αs are negative. If $A > \pi/2$, then the 45° line crosses the $\beta = \pi/2$ vertical line below A, so $\beta_1 > \pi/2$. The values of β_2 and β_3 depend on the specific value of A and the directions of the inequality are undetermined. To see this dependency let $A = \pi/2 + 2\pi$ (i.e., $n = 1$). In the same way as for $A = \pi/2$, we can obtain the ordinates of the three intersections denoted by the red dotted points in Figure

2B,

$$\beta_1^1 \simeq 2.09 > \frac{\pi}{2} \text{ at } e_1 \text{ and } \alpha_1^1 \simeq 1.19,$$

$$\beta_2^1 = \frac{5\pi}{2} \text{ at } e_2 \text{ and } \alpha_2^1 = 0, \tag{12}$$

$$\beta_3^1 \simeq 14.10 < \frac{9\pi}{2} \text{ at } e_3 \text{ and } \alpha_3^1 \simeq -0.59.$$

Notice that x_1^1 has positive real part, x_2^1 is a purely imaginary root and x_3^1 has negative real part implying that β_1^1 is in Ω_2 and β_3^1 is in Ω_1. Although it is not easy to see the location of β_3^1 in Figure 2B, it is in the shaded region.

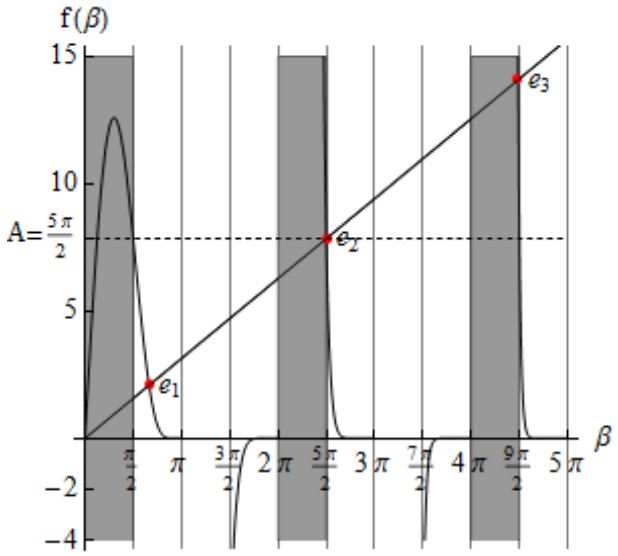

Figure 2(B). Determination of β for $A = 5\pi/2$

It is also clear in general that that if $A = \pi/2 + 2n\pi$, then the root x_{n+1}^n has zero real part, $\alpha_{n+1}^n = 0$ with imaginary part $\beta_{n+1}^n = \pi/2 + 2n\pi$. Furthermore its real part becomes positive if $A > \pi/2 + 2n\pi$ and negative if $A < \pi/2 + 2n\pi$. We summarize these results:

Lemma 1 *Delay differential equation (6) has a root with $\alpha < 0$ and $\beta \in \Omega_1$ if $\tau\gamma < \pi/2 + 2n\pi$, a root with $\alpha > 0$ and $\beta \in \Omega_2$ if $\tau\gamma > \pi/2 + 2n\pi$ and a root with $\alpha = 0$ and $\beta = \pi/2 + 2n\pi$ if $\tau\gamma = \pi/2 + 2n\pi$.*

Returning to the definition of A, the tangency condition is written as $\gamma\tau = 1/e$ on which there is a unique negative root. This is a partition curve between the real and complex roots. With a given value of γ, a small increase of τ makes $\gamma\tau > 1/e$ implying that equation (5) generates a pair of complex roots with

negative real parts. Further increases of τ may change the negative real part of λ to positive making the system unstable. Such phenomena is referred to as a *stability switch.* In order to understand the stability switch of (5), it is crucial to determine a threshold value $\tau = \tau^*$ at which the real parts of the complex roots are zero and their derivatives are positive. We then assume that $\lambda = i\upsilon$, $\upsilon > 0$, is a root of (5) for $\tau = \tau^*$. By Lemma 1, we have infinitely many solutions with the zero real parts when

$$\tau = \frac{1}{\gamma}\left(\frac{\pi}{2} + 2n\pi\right), \ n \in N \tag{13}$$

We now detect the stability switch at which the equilibrium loses stability. Since λ is a function of delay τ, we need the minimum solution of τ for which a derivative of $\lambda(\tau)$ is positive. By selecting τ as the bifurcation parameter and differentiating the characteristic equation (5) with respect to τ yield

$$(1 - \gamma\tau e^{-\lambda\tau})\frac{d\lambda}{d\tau} = \gamma\lambda e^{-\lambda\tau}.$$

which is reduced to

$$\left(\frac{d\lambda}{d\tau}\right)^{-1} = \frac{1 - \gamma\tau e^{-\lambda\tau}}{\gamma\lambda e^{-\lambda\tau}}.$$

Obtaining $e^{-\lambda\tau} = -\lambda/\gamma$ from (5) and substituting it into the last equation, we can show that the real parts are positively sensitive to a change in τ,

$$\mathrm{Re}\left[\left(\frac{d\lambda}{d\tau}\right)^{-1}\Big|_{\lambda=i\upsilon}\right] = \frac{d(\mathrm{Re}\,\lambda)}{d\tau}\Big|_{\lambda=i\upsilon} = \frac{1}{\upsilon^2} > 0.$$

This inequality implies that the real part turns to be positive from negative when τ crosses the imaginary axis.

Lemma 2 *All roots of equation (5) that cross the imaginary axis at $i\upsilon$ cross from left to right as τ increases,*

$$\frac{d(\mathrm{Re}\,\lambda)}{d\tau}\Big|_{\lambda=i\upsilon} > 0.$$

Lemmas 1 and 2 imply that the real parts of all roots are negative for $\tau < \pi/2\gamma$ and the real part of one root becomes positive when $\tau > \pi/2\gamma$. Therefore stability switch occurs when τ crosses the $\tau = \pi/2\gamma$ curve. On the other hand, it does not occur when τ crosses the $\tau = (\pi/2 + 2n\pi)/\gamma$ curve with $n > 1$. Although the real part of the root with $\beta = \pi/2 + 2n\pi$ is zero and its derivative with respect to τ is positive, there are already roots with positive real parts. Hence the threshold value of τ is

$$\tau^* = \frac{\pi}{2\gamma}$$

This result is summarized as follow:

Theorem 1 *The delay output adjustment process (3) has a threshold value τ^* of delay: The monopoly equilibrium is locally asymptotically stable for $0 < \tau < \tau^*$, locally unstable for $\tau > \tau^*$ and undergoes a Hopf bifurcation at $\tau = \tau^*$ where τ^* is the threshold value of τ defined by*

$$\tau^* = \frac{\pi}{2\alpha(a-c)}.$$

2.2 Numerical Simulations

Theorem 1 is visualized in Figure 3 where the higher hyperbolic downward sloping real curve is the locus of $\tau\gamma = \pi/2$ and the lower hyperbolic real curve is the locus of $\tau\gamma = 1/e$. The former curve divides the first quadrant of the (γ, τ) plane into two regions: the gray region in which the monopoly equilibrium is locally stable and the white region in which it is locally unstable. Although local stability (instability) implies global stability (instability) in a linear model, this is not necessarily a case in nonlinear dynamic system such as (3)[5]. Theorem 1 and the following simulations analytically and numerically confirm the birth of a periodic cycle when a parametric combination of (γ, τ) is selected from the white region of Figure 3. To examine qualitative properties of such a periodic solution, we perform three numerical simulations in which $a = 3$, $c = 1$ and $b = 1$ are fixed whereas τ and/or γ are varied.

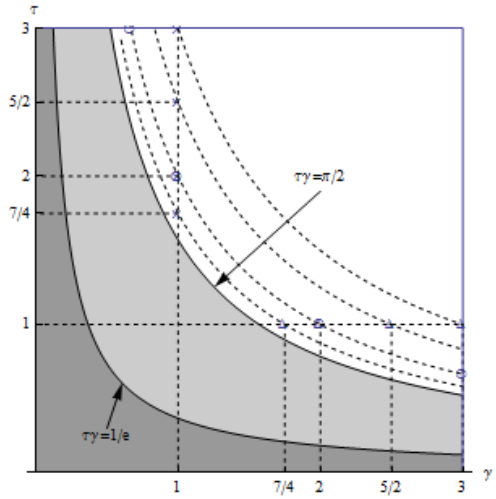

Figure 3. Division of the (γ, τ) plane into stable and unstable regions

[5] Using a logistic single species population model, which is essentially the same as the delay monopoly model (3), Wright (1955) shows global stability under the condition of $\tau < 3/2\gamma$ and presumes that his method can be used to extend the global result to $\tau < 2\pi/\gamma$. However this conjecture still remains open.

In the first simulation, we change both values of γ and τ by keeping $\tau\gamma = 2$. In particular, four different points, $(2/3, 3)$, $(1, 2)$, $(2, 1)$ and $(3, 2/3)$ are selected from the $\tau\gamma = 2$ locus. These points are in the white (unstable) region and marked by the circles in Figure 3. Numerical results with the initial function $\phi(t) = q^M - 0.1$ for $-\tau < t \leq 0$ are summarized as follows. Figure 4(A) depicts the cyclic motions of delay equation (2) in the $(q(t-\tau),\ q(t))$ plane. Note that although the four periodic motions corresponding to the different pairs of γ and τ are depicted there, only one spiral motion toward a limit cycle is observed. This implies that no matter which pair of γ and τ is selected, the phase trajectories have exactly the same periodic motion in the $(q(t-\tau),\ q(t))$ plane as far as the product of τ and γ is the same. Time trajectories of $q(t)$ from $t = 0$ to $t = 12$ are illustrated in Figure 4(B).[6] It is seen that the time trajectories have different lengths of the period but finally converge to the same periodic cycle. Observing these numerical results, we find the following:

Numerical Result 1. with fixed value of $\tau\gamma$,

1. the amplitudes of the limit cycles with different values of γ and τ are the same;
2. the time to arrive at the limit cycle becomes longer as τ becomes longer;
3. the length of a period of the cycle becomes longer as τ becomes longer.

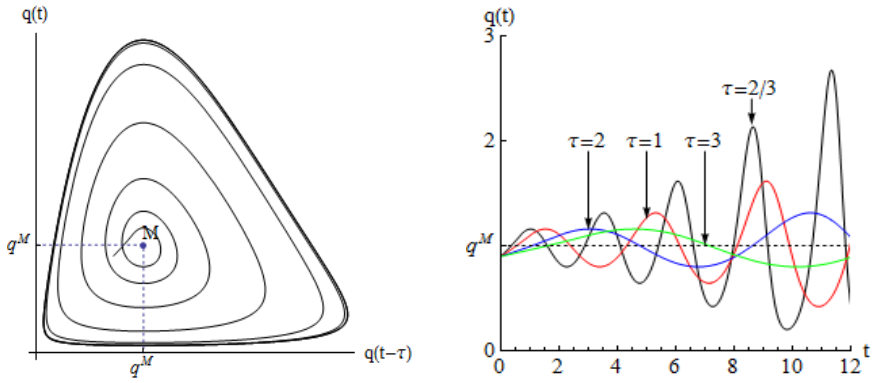

(A) Phase trajectories (B) Time trajectories

Figure 4. Numerical result in the first simulation

In the second simulation, we take four different values of τ, points $(1, 7/4)$, $(1, 2)$, $(1, 5/2)$ and $(1, 3)$ from the dotted vertical line at $\gamma = 1$, in order to detect the

[6] To prevent Figure 4(B) from getting clumsy, we limit the length of time period short. This restriction is inessential.

effect on dynamic behavior caused by changing the length of delay τ. These four points are marked by crosses in Figure 3. Figures 5(A) and 5(B) illustrate four different limit cycles in the $(q(t-\tau),\ q(t))$ plane and four different time trajectories of $q(t)$ against time between $t = 0$ and $t = 30$. Note that same color of the trajectories means same parameter specifications. The result are summarized as follows:

Numerical Result 2. As τ becomes larger with fixed value of γ,

1. the amplitude of the cycle becomes larger;
2. the arrival time to the limit cycle becomes shorter;
3. the length of a period becomes longer.

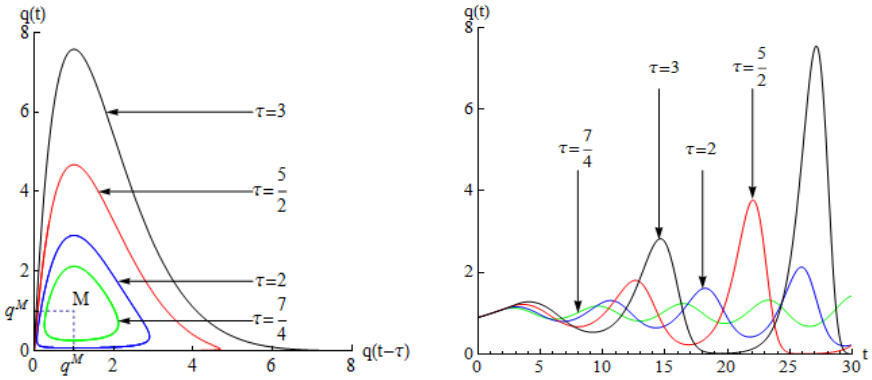

(A) Phase trajectories (B) Time trajectories

Figure 5. Numerical results in the second simulation

In the third simulation, contrary to the second one, we take four different values of γ, $(7/4, 1)$, $(2, 1)$, $(5/2, 1)$ and $(3, 1)$ from the dotted horizontal line with $\tau = 1$, in order to detect the effect on dynamic behavior caused by changing the value of γ. These four points are marked by triangles in Figure 3. Figures 6(A) and 6(B) illustrate four limit cycles in the $(q(t-\tau),\ q(t))$ plane and four time trajectories of $q(t)$ against time between $t = 0$ and $t = 30$. Note that same color of the trajectories means same parameter specifications. We have the following result:

Numerical Result 3. As γ becomes larger with fixed value of τ,

1. the amplitude of the cycle becomes larger;
2. the arrival time to the limit cycle becomes shorter;

3. the length of a period becomes longer.

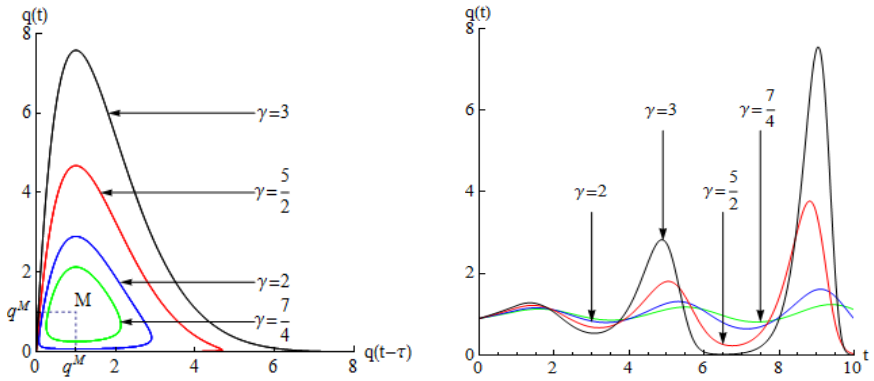

(A) Phase trajectories (B) Time trajectories

Figure 6. Numerical results in the third simulation

Theorem 1 shows that the delay equation (2) gives rise to a limit cycle when the monopoly equilibrium becomes locally unstable. Through numerical simulations, we arrive at the following results concerning the sensitivity of the cycles to changes in the parameter specifications:

Summary of Numerical Simulations

1 the amplitude of the cycle becomes larger as $\gamma\tau$ becomes larger;

2 the period of the cycle becomes longer as one of two parameters, γ and τ, becomes larger and the other is kept to be constant;

3 the convergence time to the limit cycle becomes shorter as one of two parameters, γ and τ, becomes larger and the other is kept to be constant.

3 Conclusion

We constructed a dynamic model driven by the gradient process in which a monopoly was boundedly rational and single delay was presented in the formation of the expected demand. Main analytical results were summarized in Theorem 1 in which it was demonstrated that a monopoly equilibrium was locally asymptotically stable when the delay is less than the threshold value τ^*, lost its stability when $\tau = \tau^*$ and underwent a Hopf bifurcation. We also simulated the model and numerically confirmed the following:

(N1) The monopoly equilibrium bifurcates to a limit cycle.

(N2) As the delay becomes larger, both the amplitude and the period of the cycle become larger.

Appendix

In this Appendix, we briefly summarize two different ways to solve equations (7) and (8) for α and β proposed by Frisch and Holme (1935) and Hayes (1950). Although they consider the more general characteristic equation having the form $x + B + Ae^{-x} = 0$, we apply their approaches to our simplified characteristic equation, $x + Ae^{-x} = 0$.

Frisch and Holme (1935) start with equation (8) to obtain,

$$e^{\alpha} = A\frac{\sin\beta}{\beta}$$

which can be rewritten, by using logarithms, as

$$\alpha = \log A + \log\frac{\sin\beta}{\beta}. \tag{A-1}$$

Substituting these relations into equation (7) yields

$$\beta\cot\beta + \log\frac{\sin\beta}{\beta} = \log A^{-1}. \tag{A-2}$$

Write the left-hand side by $f_{FH}(\beta)$ so that, given A, β is a solution of

$$f_{FH}(\beta) = \log A^{-1}.$$

The graphs of $f_{FH}(\beta)$ with $A = \pi/2$ and $A = 5\pi/2$ are illustrated in Figures I(A) and I(B), respectively. It appears that each graph has three intersections with the $\log A^{-1}$ line. The red points denoted as e_i correspond to the coordinates of the intersections. Their abscissas are the values of β and values of α are given by equation (A-1). It can be confirmed that the values of α and β are the same as those obtained in (11) and (12).

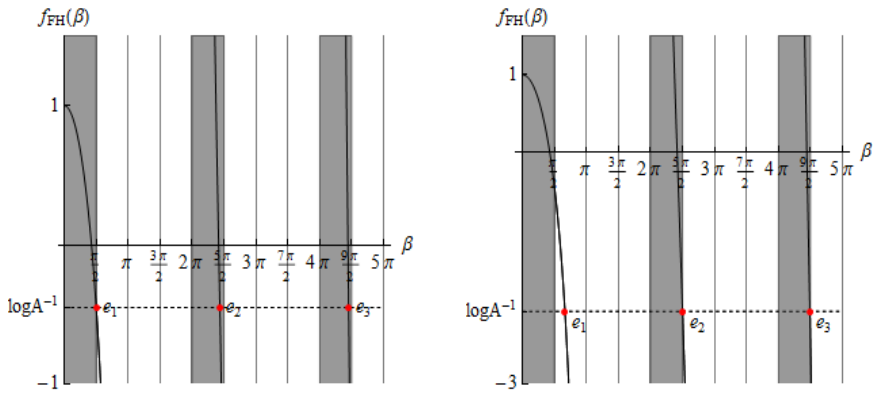

(A) $A = \pi/2$ (B) $A = 5\pi/2$

Figure I. Frisch-Holme approach

Hayes (1950) rewrites equations (7) and (8) as

$$\alpha = -Ae^{-\alpha}\cos\beta$$

and

$$\beta = Ae^{-\alpha}\sin\beta.$$

Dividing the first equation by the second and solving it for α give the real part of the root as a function of β

$$\alpha = -\beta\cot\beta \tag{A-3}$$

which is the same as equation (9). Adding up the squares of both equations and solving it for β gives the imaginary part of the root as a function of α

$$\beta = \sqrt{A^2e^{-2\alpha} - \alpha^2}. \tag{A-4}$$

The right hand sides of (A-3) and (A-4) will will be denoted as $f_H(\beta)$ and $g_H(\alpha)$. The $\alpha = f_H(\beta)$ curve is positive-sloping and the $\beta = g_H(\alpha)$ curve is negative sloping in Figures II(A) and II(B). The β-values of the intersections of these two functions are the solutions of $\beta = g_H(f_H(\beta))$ and the α-values are given by $\alpha = f_H(\beta)$. The good point of his approach is that the intersections are the coordinates in the complex plane. So it is easy to see whether the real part is negative or positive. The values of α and β at the intersections are the same as those given in (11) and (12).

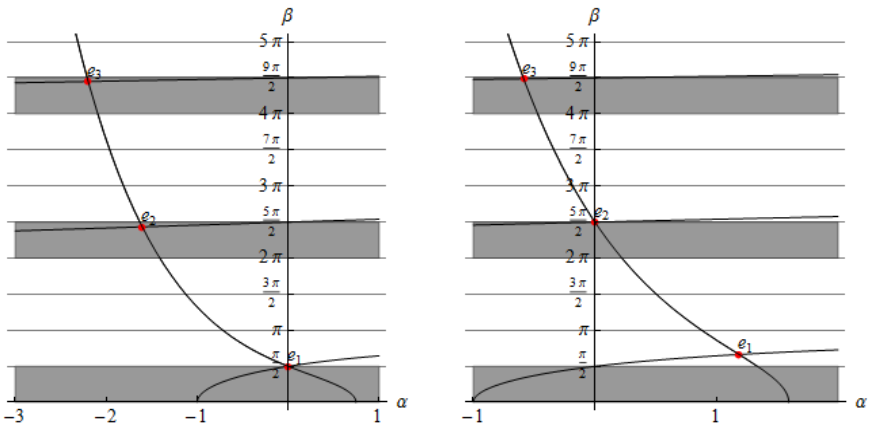

(A) $A = \pi/2$ (B) $A = 5\pi/2$

Figure II. Hayes approach

References

[1] Frisch, R., and H. Holme, "The Characteristic Solutions of a Mixed Difference and Differential Equation Occuring in Economic Dynamics," *Econometrica*, 3 (1935), 225-239.

[2] Hayes, N. D., "Roots pf the Transcendental Equation Associated with a Certain Difference-Differential Equation," *Journal of the London Mathmatical Society*, 25 (1950), 226-232.

[3] Invernizzi, S., and A. Medio, "On Lags and Chaos in Economic Dynamic Models," *Journal of Mathematical Economics*, 20 (1991), 521-550.

[4] Matsumoto, A., "Note on Goodwin's 1951 Nonlinear Accelerator Model with an Investment Lag," *Journal of Economic Dynamics and Control*, 33 (2009), 832-842.

[5] Matsumoto, A., and F. Szidarovszky, "Delay Differential Neoclassical Growth Model," *Journal of Economic Behavior and Organization,* 78 (2011a), 272-289.

[6] Matsumoto, A., and F. Szidarovszky, "An Elementary Study of a Class of Dynamic Systems with Single Time Delay," DP 161 (http://www2.chuo-u.ac.jp/keizaiken/discuss.htm), Institute of Economic Research, Chuo University, (2011b).

[7] Naimzada, A., "A Delay Economic Model with Flexible Time Lag," *mimeo*, 2011.

[8] Puu, T. *Attractors, Bifurcations and Chaos*, 2003, Berlin/Heidelberg/New York, Springer-Verlag.

[9] Wright, E. M., "On a Class of Prey-Predator Population Models with Time Lag," *Acta Mathematica Applicatae Sinica*, 11 (1955), 12-21.